FEDERAL UNIVERSITY OF TECHNOLOGY, AKURE
JOURNAL OF ENGINEERING AND ENGINEERING TECHNOLOGY

MODELLING AND SIMULATION OF FAULTS AND FAULT LOCATION DETECTOR FOR RADIAL DISTRIBUTION SYSTEM

[1]Oji, I. C., [1]Ale, T. O. and [2]Odeyemi, C. S.

[1]Department of Electrical and Electronics Engineering, Federal University of Technology, Akure, Nigeria
[2]Department of Computer Engineering, Federal University of Technology, Akure, Nigeria
**Correspondence: sent2charlly@gmail.com*

Oji, I. C., Ale, T. O. and Odeyemi, C. S. (2025): Modelling and Simulation of Faults and Fault Location Detector for Radial Distribution System. *FUTA Journal of Engineering and Engineering Technology /19(1), 1-11*

Received Date: 15.06.24 **Accepted Date: 10.08.24**

Abstract
Distribution lines are always exposed to the environment due to their network configuration and this makes its possibility of fault occurrence to be very high. Fault, as a regular incidence on distribution power system, can lead to failure of equipment, fire outbreak, power instability and other forms of hazardous conditions causing huge financial loss and increased system downtime. To avoid these conditions, it is necessary to detect and locate the fault on the network as fast as possible so as to prevent power system damages and reduce system downtime. This study designed a fault location system model that can detected and located three-phase faults at the point of occurrence using a developed 33 kV Ubulu-Uku radial distribution system as a test feeder. Thereafter, fault location equations were formulated which resulted into one single equation for three-phase fault on the network. An impedance-based algorithm was designed which was used to detect and locate fault on the distribution line. The designed algorithm was evaluated using varying line impedances of 0.01 Ω, 0.15 Ω, 0.35 Ω, 0.5 Ω and 0.65 Ω which produced faults located along path 6 section 17, path 8 section 21, path 8 section 21, path 4 section 12 and path 8 section 21 with fault distances of 3.72 km, 3.93 km, 4.03 km, 4.81 km, and 4.21 km respectively from the main substation. The overall percentage accuracy of the designed model was found to be 86 %. The results presented show performance of the designed algorithm. Encouraging the implementation of this study can improve fault location accuracy, reduce response time, lower maintenance cost and minimize supply interruptions.

Keywords: *Faults, Distribution network, Fault location, Impedance-based algorithm.*

Introduction

Faults on electric power lines may be seen as sudden disturbance that can cause abnormal flow of current in the lines, be it transmission or distribution lines (Mbamaluikem et al., 2018) and can lead to an unexpected change in the system parameter (Hazarika and Roy, 2021). They are common occurrence, and constantly induced by short circuits, switching operations and lightning cases, equipment failures, weather events, physical damage to power lines such as accidents, vandalism or other issues (Oji et al, 2024). However, faults need to be detected and located first, in order to send maintenance crews to fix it before restoration. Locating faults in a radial distribution system is not an easy task because of its non-linearity of the system, high complexity of the network, system difficulty caused by fault resistance, and load uncertainty (Mohammed and Ali, 2010), so when fault occurs, it affects the whole distribution network making fault location, fault clearing and restoration a difficult task to do. The great majority of today's electric power company's maintenance crews have for several years located faults through receiving trouble calls from affected customers and visual inspection (Oji et al., 2024). These faults need to be detected, located and cleared in due time, not by the traditional way of receiving trouble calls from the affected customers but by use of advanced technological methods such as remote sensing and fault location technologies through the use of advance software to monitor, control and analyze real-time data from the network to quickly locate fault and isolate the faulty system.

In recent years, several fault location methods for transmission and distribution have been proposed solve these problems. In Ale and Saliu (2017), the use of special properties of travelling discrete wavelet transforms to differentiate between faults

occurring along different laterals was presented. This method is mostly suitable for high voltage transmission lines and very long distribution networks but characterized by decreased accuracy for network with smaller distances. Also, a method which uses generated signals of voltage and current measured at two terminal ends of the distribution system was presented by Hizan and Crossley (2012). The limitation was that the method did not consider a distribution network with many laterals and sub-laterals. Also, the use of voltage sag pattern in locating fault was researched into by Awalin et al. (2012) with the use of phasor angle of faulted sections. This method was used for large distribution lines of distance greater than 70 km (> 70 km) with multiple measurements making it unsuitable for distribution system with smaller distances and real-time limited measurement values thereby reducing its accuracy in locating fault. Hamid et al. (2021), also developed an algorithm which was implemented on a Smart Feeder Meter to locate fault using its equivalent load impedance which was simulated on MATLAB. In the method used, the focus was on the secondary (low voltage side) distribution network. The method is not cost-effective because it requires Smart Feeders Meters (SFM) to be installed at every distribution substation point on the network. Intelligence-based methods such as Artificial Neural Network (ANN) by Mbamaluikem et al. (2018), and Hybrid classifier method by Jemali et al. (2020) as proposed in their research, was used to detect, recognize and analyzed faults on active distribution networks, made use of large information and data obtained from past fault records of the network but its major drawback is that it needs to be trained and retrained at any circumstance of the network which increases complexity of the method, and for distribution network with smaller distances and limited real-time measurement, the method may not give accurate result because the more the data obtained and trained, the higher the level of accuracy. In Kulikov et al. (2023), the use of high frequency components of currents and voltage was presented using the generated harmonics from the instantaneous values of phase current and voltage from the two node ends of overhead power lines during short circuit to determine and detect the relative value of the distance from the main substation to the short circuit location and locate faults in an automated distribution network. The drawback of this method is that the harmonics generated from the current and voltage were not filtered to reduce the effect of noise and undesirable harmonic components thereby affecting the accuracy of the fault location with considerable error in its desired distance estimation. However, these methods do not consider active distribution system with shorter distances, more laterals and sub-laterals on the network, and real-time limited measurement values determined from the terminals of the distribution injection substation. In this paper, impedance-based method of estimating fault location and distance of 3-phase fault for active radial distribution lines for shorter distances (usually with a total line distance less than 50 km) was utilized.

Distribution systems are typically composed of a main feeder, several laterals and sub laterals with different length with the use of overhead cable making the system exposed to fault at different location on the system. To determine the location and distance of fault accurately and effectively from the injection substation, a mathematical modeled equation, which made use of voltage, current and impedance measured from the main substation, was developed to obtain the fault

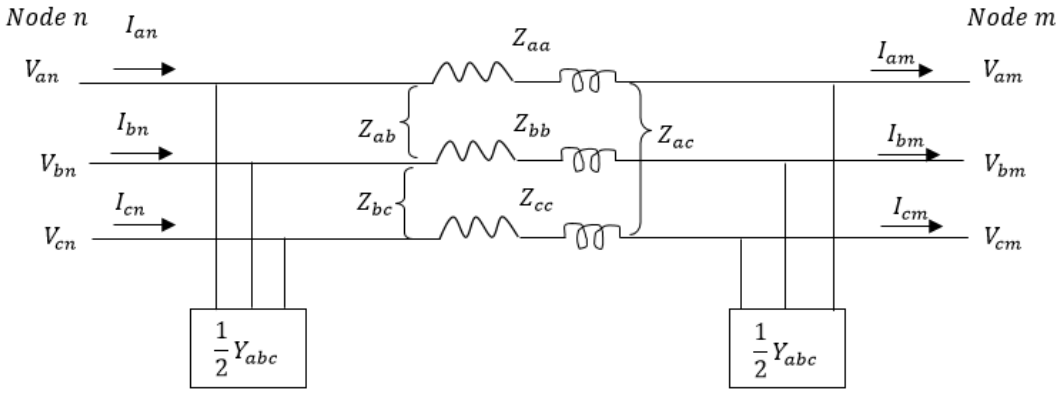

Figure 1: Three-phase exact line segment model (Oji *et al*, 2024)

parameters, and locate the fault points on the system so as to speed up the restoration process when fault occurs and improve service reliability. A distribution line can be represented by a line model section as seen in Figure 1.

Using Kirchoff's voltage and current law, the general equation defining the *output* node m and input node n voltage and current are given in Equation 1

$$\begin{bmatrix} V_{abc} \\ I_{abc} \end{bmatrix} m = \begin{bmatrix} d & -b \\ -c & a \end{bmatrix} \cdot \begin{bmatrix} V_{abc} \\ I_{abc} \end{bmatrix} n \quad (1)$$

The a, b, c, d parameters in Equation 1 are defined in Equations 2, 3, and 4 as

$$a = d = I + 0.5\, x^2\, Z_{abc}\, Y_{abc} \quad (2)$$

$$b = x\, Z_{abc} \quad (3)$$

$$c = x\, Y_{abc} + 0.25\, x^3 \cdot Y_{abc}\, Z_{abc}\, Y_{abc} \quad (4)$$

where I is the third order identity matrix, Z_{abc} is the line series impedance in (Ω/km), Y_{abc} is the shunt admittance in Ω^{-1}/km, x is the length of the line in m

For a fault located in *x* kilometer from the beginning of the line, the fault voltage V_f and current can be rewritten from Equation 1 and expressed as seen in Equations 5 and 6

$$V_f = d_x\, V_n - b_x\, I_n \quad (5)$$

$$I_f = I_u - I_L \quad (6)$$

where V_f is fault voltage as seen on the line, V_n is the bus voltage, I_n is the bus current, I_f is the fault current, I_u is $-c_x\, V_{sk} + a_x\, I_{sk}$ and it is the current magnitude as seen on the line during fault while I_L is the pre-fault current

Proposed 3-Phase Fault Location Equation

Faults, as an abnormal condition in the distribution system, can present itself as three-phase (3-ϕ) or three phase – to – ground (3-ϕ_g) faults (Prajapat, 2020).

Considering Figure 2 which presents the most general ground fault. The voltage and current relation at the fault point for this model is given by Equation 7.

$$\begin{bmatrix} V_{fa} \\ V_{fb} \\ V_{fc} \end{bmatrix} = \begin{bmatrix} Z_{fa} + Z_{fg} & Z_{fg} & Z_{fg} \\ Z_{fg} & Z_{fb} + Z_{fg} & Z_{fg} \\ Z_{fg} & Z_{fg} & Z_{fc} + Z_{fg} \end{bmatrix} \begin{bmatrix} I_{fa} \\ I_{fb} \\ I_{fc} \end{bmatrix} \quad (7)$$

where $V_{f\,(abc)}$ is the fault point voltage at phase a, b, c (in volt), $I_{f\,(abc)}$ is the fault current on phase a, b, c (in amps), and $Z_{a,b,c\text{-}g}$ is fault impedance at phase a, b, c and ground (in ohms).

From Equation 7, it will be seen that only the faulted phase has fault current that is non-zero ($I_f \neq 0$). Replacing Equation 7 into Equation 5, each faulted phase can be written as seen in Equation 8 and the coefficients M_k and N_k in Equation 8 are defined and expressed in Equation 9 as;

$$\begin{aligned} Z_{f_k} \cdot I_{f_k} + Z_{f_g} \cdot I_{f_k} &= 0.5\left[Z_{abc} \cdot Y_{abc} \cdot V_{n_k}\right]x^2 \\ &\quad - \left[Z_{abc} \cdot I_{n_k}\right]x + V_{n_k} \\ &= 0.5\, M_k\, x^2 - N_k\, x + V_{n_k} \end{aligned} \quad (8)$$

$$M_k = \begin{bmatrix} Z_{aa} & Z_{ab} & Z_{ac} \\ Z_{ba} & Z_{bb} & Z_{bc} \\ Z_{ca} & Z_{cb} & Z_{cc} \end{bmatrix} \cdot \begin{bmatrix} Y_{aa} & Y_{ab} & Y_{ac} \\ Y_{ba} & Y_{bb} & Y_{bc} \\ Y_{ca} & Y_{cb} & Y_{cc} \end{bmatrix} \cdot \begin{bmatrix} V_{n_a} \\ V_{n_b} \\ V_{n_c} \end{bmatrix};$$

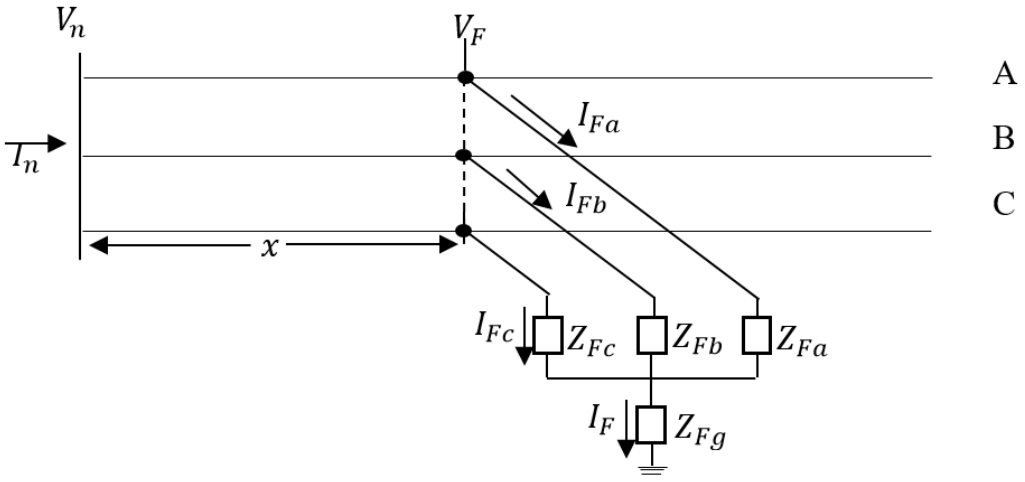

Figure 2: Distribution line subjected to ground fault (Oji *et al*., 2024)

$$N_k = \begin{bmatrix} Z_{aa} & Z_{ab} & Z_{ac} \\ Z_{ba} & Z_{bb} & Z_{bc} \\ Z_{ca} & Z_{cb} & Z_{cc} \end{bmatrix} \cdot \begin{bmatrix} I_{n_a} \\ I_{n_b} \\ I_{n_c} \end{bmatrix} \quad (9)$$

When expanding Equation 8, it will result in *n* equations existing in their complex form where *n* represents the total number of faulted phases and by conducting algebraic operations involving complex algebra, the fault location equation for a three-phase-to-ground and three-phase fault can finally be written as expressed in Equation 10.

$$\left[0.5 \sum_{k\in\Omega_k} \{M_k \cdot I_{f_k}^*\}\right] x^2 - \left[\sum_{k\in\Omega_k} \{N_k \cdot I_{f_k}^*\}\right] x + \left[\sum_{k\in\Omega_k} \{V_{n_k} \cdot I_{f_k}^*\}\right] = 0 \quad (10)$$

Equation 10 becomes the Generalized 3-phase Fault Location Equation which is used to estimate the possible fault distance equation by using the 3-phase voltages and current measured at the substation, the line parameters and also the fault current. These variables are used to calculate the coefficients *M* and *N* in Equation 10 considering its computations obtained from Equation 9.

EquationSectional Fault Distance

The formulated fault location equation expressed in Equation 10 is a second-order polynomial used in obtaining the equation of fault distance *x* within a known faulty section which was formulated and then further simplified and expressed in Equation 11.

$$\beta_2 x^2 + \beta_1 x + \beta_0 = 0 \quad (11)$$

where β_0, is a constant while β_1, and β_2, are the coefficients of *x* and x^2 respectively and can be obtained from Equation 12.

$$\begin{cases} \beta_2 = 0.5\, M_k\, I_f \\ \beta_1 = I\, N_k\, I_f \\ \beta_0 = V_n\, I_f \end{cases}; \quad (12)$$

he fault distance, *x*, within a known faulty section, which is formulated through Equation 11 for both three-phase-to-ground and three-phase fault, represents the physically correct solution and can be calculated using Equation 13.

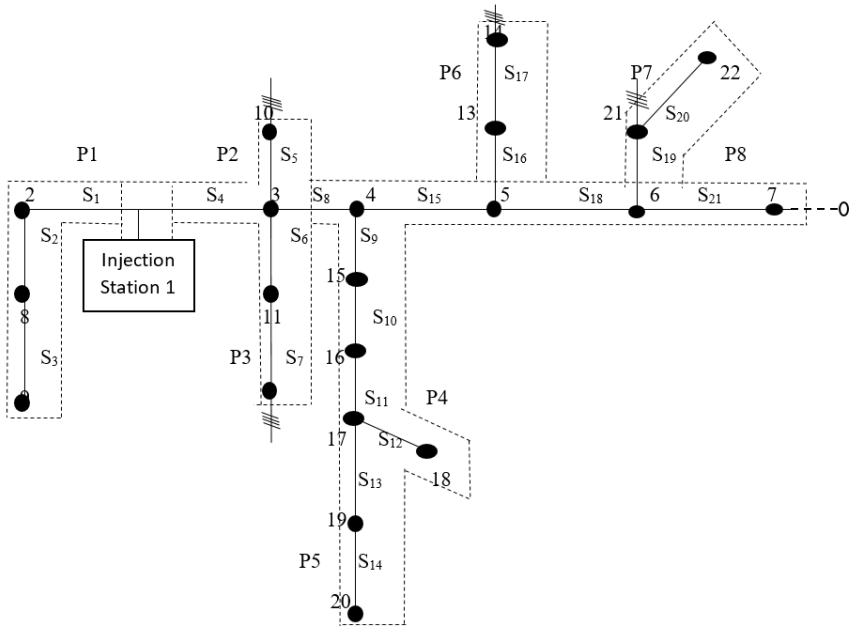

Figure 3: One-line diagram of Ubulu – Uku Distribution Feeder Network

$$x = \begin{cases} \frac{-\beta_1 + \sqrt{{\beta_1}^2 - 4\beta_2\beta_0}}{2\beta_2} & \beta_1 > 0 \\ \frac{-\beta_1 - \sqrt{{\beta_1}^2 - 4\beta_2\beta_0}}{2\beta_2} & \beta_1 < 0 \end{cases} \quad (13)$$

The evaluation of the physically correct fault distance requires obtaining the fault distance of the fault point from the main substation. This is possible because all the sections in the radial distribution network are unique with their line parameters and having different distances. Also, every section has its sending-end and receiving-end nodes. Having determined the fault point within a faulty section, the fault distance (F_d) from the main substation can be determined as expressed in Equation 14

$$F_d = D + x \quad (14)$$

where F_d is the fault distance from the main substation, D is the route length to the sending-end node of the faulty section, *x* is the fault distance within the faulty section.

Method

The methodology for this research involved the use of a 22-node, 33 kV Ubulu-Uku radial distribution feeder in Ogwashi-Uku region of Delta State, Nigeria as a test feeder as seen in Figure 3. The entire feeder network in Figure 3, with a total length of 34.12 km with 6 main laterals, and a yet-to-be energized substation point for a possibility of future expansion, was sectionalized into 21 sections and 8 power flow paths. The line length in each section, sections that made up each path and their corresponding route length are presented in Tables 1 and 2.

Table 1: Network's sectional span

Sections	Bus		Distance	Sections	Bus		Distance
	From	To	D (km)		From	To	D(km)
1	1	2	0.65	12	17	18	0.85
2	2	8	0.35	13	17	19	2.50
3	8	9	0.75	14	19	20	0.75
4	1	3	1.60	15	4	5	0.85
5	3	10	1.05	16	5	13	0.77
6	3	11	0.65	17	13	14	0.35
7	11	12	0.85	18	5	6	1.10
8	3	4	0.25	19	6	21	0.45
9	4	15	0.50	20	21	22	0.80
10	15	16	0.60	21	6	7	1.20
11	16	17	1.40				

Table 2: Section, sectional distance and route length of power flow path

Path	Section and Sectional Distance (km)	Route Length (km)
P1	Section 1 (0.65); Section 2 (0.35); Section 3 (0.75)	1.75
P2	Section 4 (1.60); Section 5 (1.05)	2.65
P3	Section 4 (1.60); Section 6 (0.65); Section 7 (0.85)	3.10
P4	Section 4 (1.60); Section 8 (0.25); Section 9 (0.50); Section 10 (0.60); Section 11 (1.40); Section 12 (0.85)	5.20
P5	Section 4 (1.60); Section 8 (0.25); Section 9 (0.50); Section 10 (0.60); Section 11 (1.40); Section 13 (2.50); Section 14 (0.75)	7.55
P6	Section 4 (1.60); Section 8 (0.25); Section 15 (0.85); Section 16 (0.77); Section 17 (0.35);	3.82
P7	Section 4 (1.60); Section 8 (0.25); Section 15 (0.85); Section 18 (1.10); Section 19 (0.45); Section 20 (0.80)	5.05
P8	Section 4 (1.60); Section 8 (0.25); Section 15 (0.85); Section 18 (1.10); Section 21 (1.20)	5.00
Total distance		**34.12**

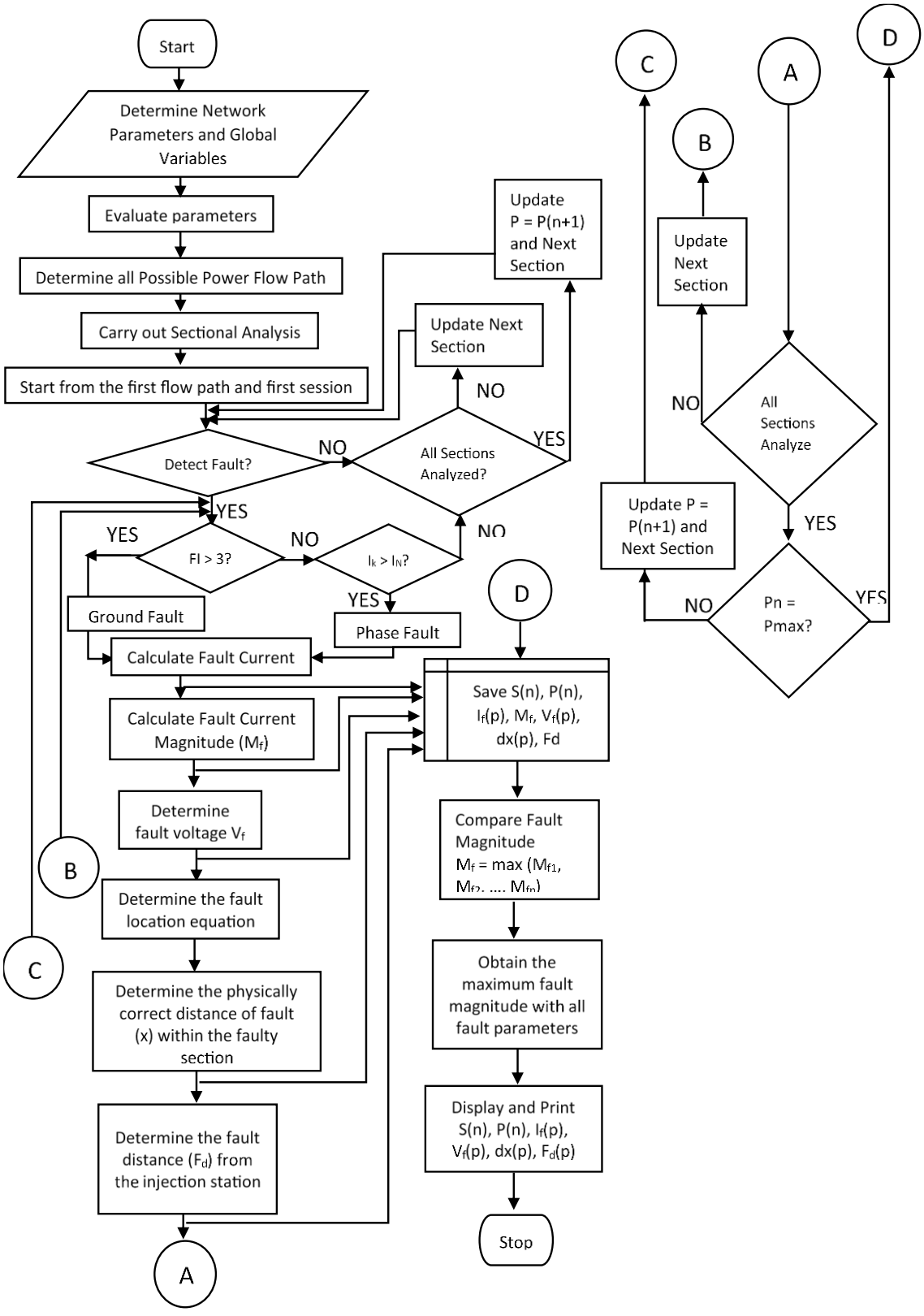

Figure 4: Developed flowchart of Impedance-based fault location

Fault Detection and Classification

Fault detection is an important step in the fault location procedure and the task include the creation of fault classification index, FI, which is used as the indicator, and the design of a decision rule to detect and classify the faulty type (Oji *et al*, 2024). The magnitude of the phase impedance a, b, c, the average magnitude of phase impedance Z_A, and the

normalized phase impedance Z_{N_k} were obtained as expressed in Equations 15 to 17.

$$\begin{cases} Z_a = \frac{V_a}{I_a} \\ Z_b = \frac{V_b}{I_b} \\ Z_c = \frac{V_c}{I_c} \end{cases} \quad (15)$$

$$Z_A = \frac{Z_a + Z_b + Z_c}{3} \quad (16)$$

$$\begin{cases} Z_{N_a} = \left|\frac{Z_a}{Z_A}\right| \\ Z_{N_b} = \left|\frac{Z_b}{Z_A}\right| \\ Z_{N_c} = \left|\frac{Z_c}{Z_A}\right| \end{cases} \quad (17)$$

Similarly, the phase current and the normalized phase current was also be obtained by applying Equations 18 and 19.

$$I_A = \frac{I_a + I_b + I_c}{3} \quad (18)$$

$$\begin{cases} I_{N_a} = \left|\frac{I_a}{I_A}\right| \\ I_{N_b} = \left|\frac{I_b}{I_A}\right| \\ I_{N_c} = \left|\frac{I_c}{I_A}\right| \end{cases} \quad (19)$$

where $I_{a,b,c}$, is current phasor quantities in phase a, b, c, $Z_{a,b,c}$, is phase impedances in phase a, b, c, $Z_{Na,b,c}$ is the normalized impedances of phase a, b, c, and $I_{Na,b,c}$ is the normalized currents of phase a, b, c.

As a result of these, fault classification index, FI, which can be used for both three-phase-to-ground and three-phase faults, was formulated as expressed in Equation 20.

$$FI_{abc}, FI_{abc-g} = \left(1 - Z_{N_a}\right) + \left(1 - Z_{N_b}\right) + \left(1 - Z_{N_c}\right) \quad (20)$$

Similarly, the decision rule was designed with the following classifications;

(a) If FI < 3 and $|I_k| < I_N$, distribution feeder is normal

(b) If FI > 3, the fault is seen as three-phase – to – ground fault

(c) If FI < 3 and $|I_k| > I_N$, the fault is seen as three-phase fault

Fault Location Algorithm

A step-by-step fault location algorithm, which accounts for both lateral and sublateral distribution system, was designed for the implementation of locating faults in radial distribution system and is presented as flowchart in Figure 4.

Fault Distance Accuracy

The percentage accuracy of the fault distance was calculated as the ratio of the simulated distance to the distance from the main substation to the end of the faulty section as expressed in Equation 21.

$$Percentage\ (\%)\ accuracy = \frac{d_{sim}}{T_d} \times 100 \quad (21)$$

where d_{sim} is the MATLAB simulated line distance obtained from the main substation to the faulty point of the faulty line section and T_d is the total distance obtained from the main substation to the end of the faulty line section.

After calculating the percentage accuracy for each fault distance, the average percentage accuracy of the designed algorithm was obtained as the ratio of the sum of individual percentage accuracy for each of the fault distance to the number of sections in the feeder network. This is expressed in Equation 22.

$$Average\ \%\ accuracy = \frac{\sum Individual\ \%\ accuracy\ for\ each\ fault\ type}{Number\ of\ sections\ in\ the\ feeder\ network} \quad (22)$$

Results and Discussion

The results presented in this section were obtained having evaluated the designed algorithm with the real-time line and load parameters of the 22-node 33 kV Ubulu-Uku distribution feeder which was used as the test feeder. These results were obtained by varying the values of the line impedance across each of the 21 sections that made up the distribution feeder. The various values of the line impedance used for the test feeder were 0.01 Ω, 0.15 Ω, 0.35 Ω, 0.50 Ω and 0.65 Ω, and each of them produced different fault magnitude both in three-phase – to – ground (3 - ϕ-g) fault and three – phase (3 - ϕ) fault for each of the 21 sections of the test feeder. These fault magnitudes are presented in Figures 5 to 9. The graph of the fault magnitude displayed shows how severe the impact of fault is in each of the 21 sections of the test feeder. As a result of the highest fault magnitude obtained in the above figures due to varying line impedances, the fault distances from the main substation to the fault point obtained were 3.72 km, 3.93 km, 4.02 km, 4.81 km and 4.21 km respectively with their corresponding fault distance analysis displayed in Table 3 showing line impedance (ZL), fault magnitude (Mf), faulty section, sectional span (Sp in km), route length (RL in km), fault current (If), fault voltage (Vf), sectional fault distance (x in km), fault distance from the main substation (Fd in km) and its operational status.

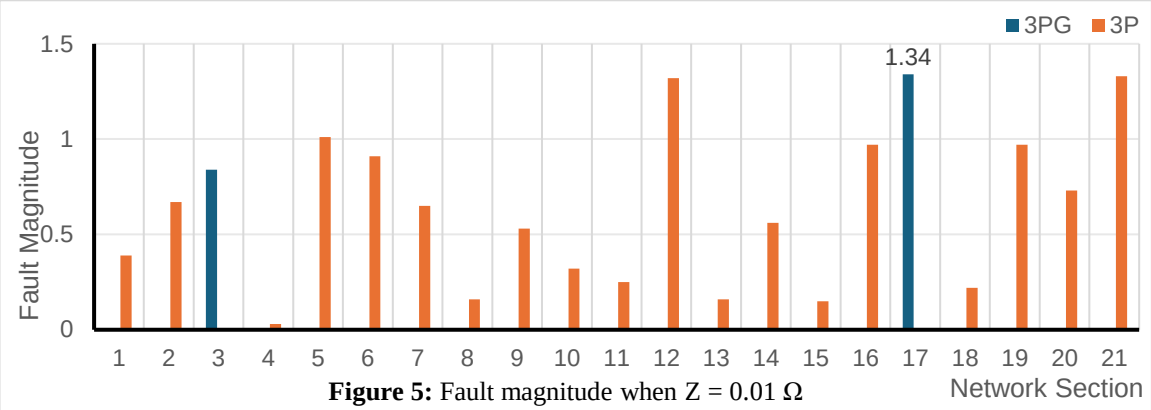

Figure 5: Fault magnitude when Z = 0.01 Ω

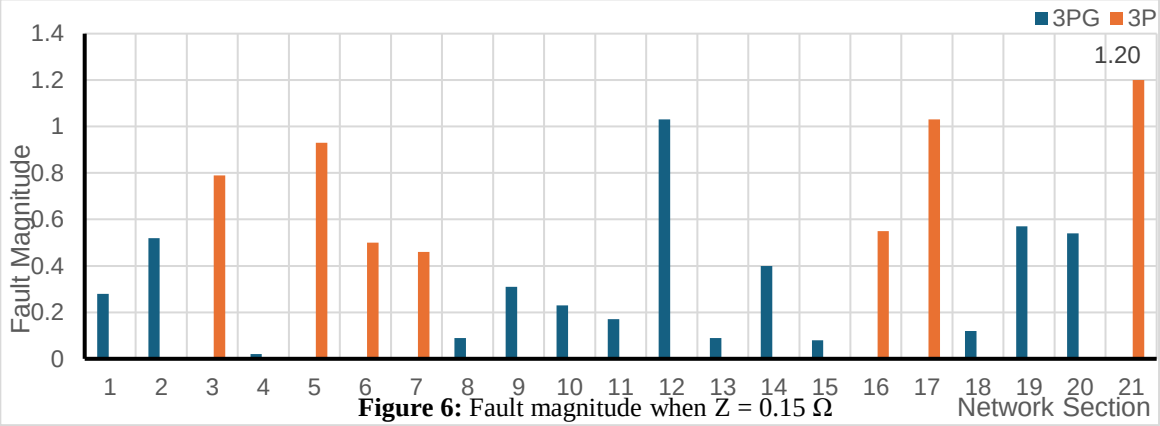

Figure 6: Fault magnitude when Z = 0.15 Ω

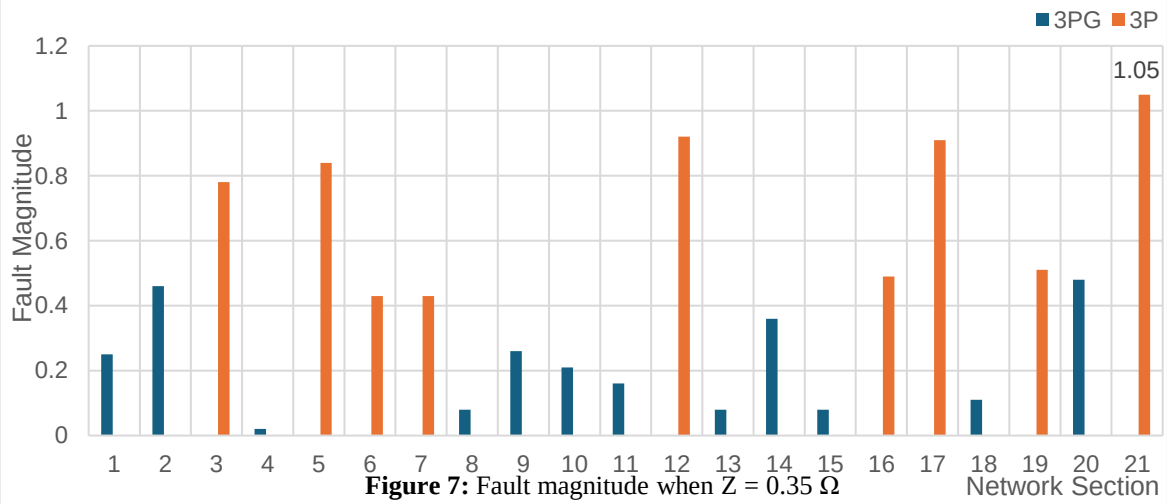

Figure 7: Fault magnitude when Z = 0.35 Ω

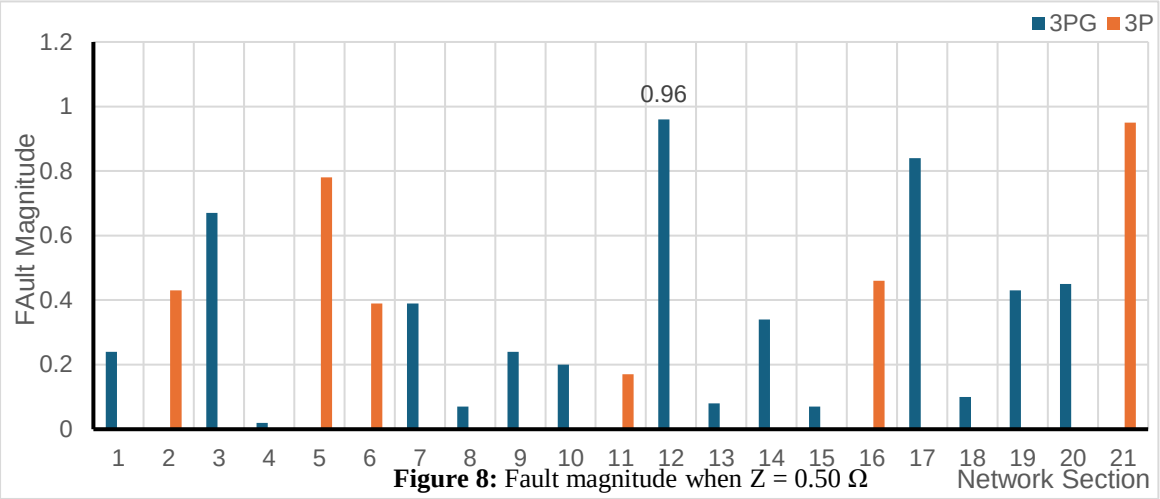

Figure 8: Fault magnitude when Z = 0.50 Ω

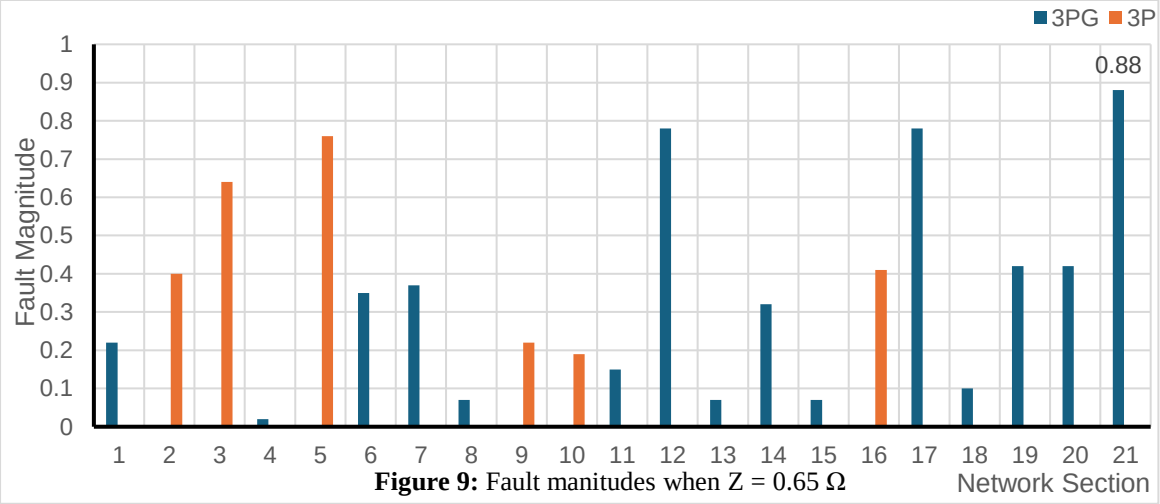

Figure 9: Fault manitudes when Z = 0.65 Ω

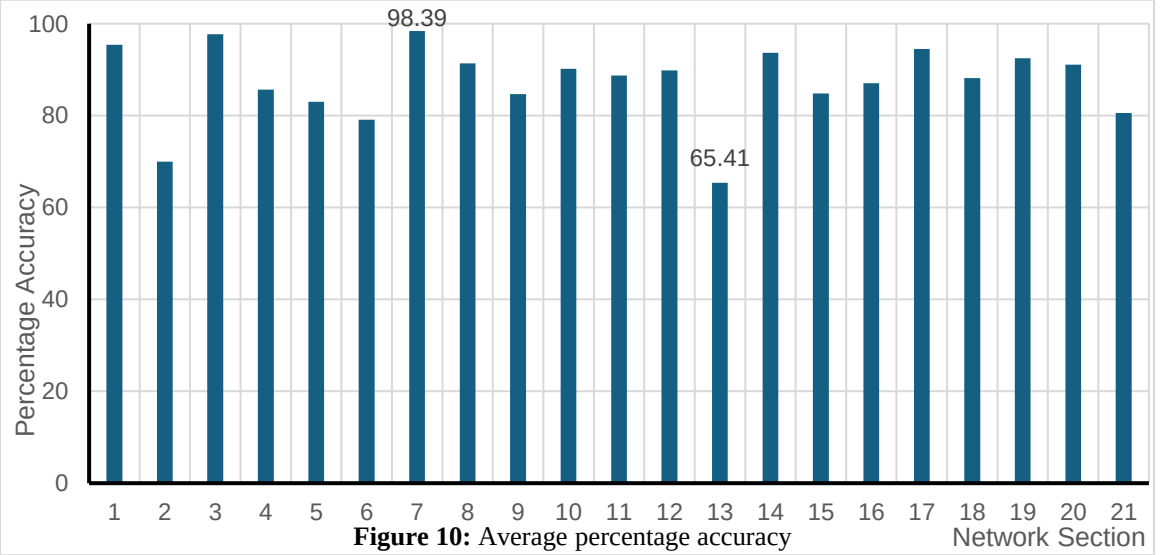

Figure 10: Average percentage accuracy

The percentage accuracy of fault distance for the analyzed fault distance analysis from the main substation to the end of each of the faulty section is presented in Table 4. The average percentage accuracy for the simulated fault distances across the 21 sections showing their average minimum and maximum percentage accuracy is presented in Figure 10. The graph of the average percentage accuracy presented provides a single percentage value for each of the sections on the network for

each analyzed fault type and it represents how accurate, on the average, are the fault distances obtained.

Table 3: Fault distance analysis

Z_L (Ω)	M_f	Path	Faulty Section	Sp (km)	R_L (km)	I_f (A)	V_f (V)	x (km)	F_d (km)	Operational Status
0.01	1.34	6	17	0.35	3.82	0.68	1.45	0.25	3.72	3-ϕ_g
0.15	1.20	8	21	1.20	5.00	0.72	1.35	0.13	3.93	3-ϕ
0.35	1.05	8	21	1.20	5.00	0.63	1.55	0.22	4.02	3-ϕ
0.50	0.96	4	12	0.85	5.20	0.51	1.93	0.46	4.81	3-ϕ_g
0.65	0.88	8	21	1.20	5.00	0.53	1.86	0.41	4.21	3-ϕ_g

Table 4: Percentage accuracy of analyzed fault distances

Path	Section	Simulated Distance (km)	Total faulty distance (km)	Percentage Accuracy (%)
6	17	3.72	3.82	97.38
8	21	3.93	5.00	78.60
8	21	4.03	5.00	80.60
4	12	4.81	5.20	92.50
8	21	4.21	5.00	84.22

Conclusion

This paper presents a typical radial distribution feeder network which was used as a test feeder to determine and locate faults on it using its three-phase load and line parameters as pre-fault values and then evaluated on the designed algorithm. The results presented from the evaluation of the algorithm show that the average minimum percentage accuracy was found to be 65.41 % in path 5 section 13 while the average maximum percentage accuracy was found to be 98.39 % in path 3 section 7. The overall average percentage accuracy of the designed algorithm was obtained to be 86 %. The performance of the designed algorithm gives a reasonable accurate value with encouraging results for practical implementation.

This paper presents a typical radial distribution feeder network which was used as a test feeder to determine and locate faults on it using its three-phase load and line parameters as pre-fault values and then evaluated on the designed algorithm. The results presented from the evaluation of the algorithm show that the average minimum percentage accuracy was found to be 65.41 % in path 5 section 13 while the average maximum percentage accuracy was found to be 98.39 % in path 3 section 7. The overall average percentage accuracy of the designed algorithm was obtained to be 86 %. The performance of the designed algorithm gives a reasonable accurate value with encouraging results for practical implementation.

References

Ale, T. O., and Saliu, R. A., (2017): Fault Detection on High Voltage Transmission lines using Discrete Wavelet Transform, *Journal of Emerging Trends in Engineering and Applied Science*, 8 (3), 136 – 142.

Awalin, L.J, Mokhlis, H., and Halim A.H.A, (2012): Improved Fault Location on Distribution Network Based on Multiple Measurement of Voltage Sags Pattern, In Proceedings at the *IEEE International Conference on Power and Energy* (PECon), Kota Kinabalu, Malaysia, 2 – 5 December, 767 – 772.

Hamid M., Rahman D., Karsten H., and Hamid R. S., (2021): Real Fault Location in a Distributed Network using Smart Feeder Meter Data, *Energies* 2021, 14, 3242, 1 – 16.

Hazarika J., and Roy O.P., (2021): Distribution System Fault Analysis using MATLAB / SIMULINK, *Intelligent Computing and Technologies Conference*, ICTCon2021, 1 – 8.

Hizan, H., and Crossley, P. A., (2012): Single-Ended Fault Technique on Radial Network using Fault Generated Current Signal, *IEE Transaction on Power Delivery*, 19 (2), 153 – 161.

Oji, I. C., Ale, T. O., Odeyemi, C. S., Dare-Adeniran, I. O., Aliyu, O. A., (2024): Development of Smart Ground Fault Location Model for Radial Distribution System, *International Journal of Innovative Science and Research Technology*, 9 (4), 2456 – 2165, 2982 – 2995.

Jameli, S., Bahmanya, A., and Ranjbar, S., (2020): Hybrid Classifier for Fault Location in Active Distribution System, *Protection and Control of Modern Power System*, 1 - 9.

Kulikov A., Ilyushin P., Suslov K., and Filuppov S., (2023): Estimating the Error of Fault Location on Overhead Power Lines by Emerging State Parameters using an Analytical Technique, *Energies* 2023, 16, 1552.

Mbamaluikem P.O., Olabode O.R., and Adedokun A.G., (2018): Artificial Neural Network Based Smart Shunt Fault Recognition System for the 33kV Nigerian Power lines, In Proceedings at the *1st International Conference and Exhibition on Technological Innovation and Global Competitiveness of Federal Polytechnic*, Ilaro, 5 – 8 November, 1 – 7.

Mohammed A. M., and Ali, A.A., (2010): A Novel Fault Locator System; Algorithm, Principle and Implementation, *IEEE Transaction on Power Delivery*, 25 (1), 35 – 46.

Prajapat D. (2020), Faults and Effects in Electrical Power Systems, Madhav University Publication, India.